



# Plant carbon allocation drives turnover of old soil organic matter in permafrost tundra soils

Lorna E. Street<sup>1</sup> | Mark H. Garnett<sup>2</sup> | Jens-Arne Subke<sup>3</sup> | Robert Baxter<sup>4</sup> | Joshua F. Dean<sup>5</sup> | Philip A. Wookey<sup>3</sup>

<sup>1</sup>School of Geosciences, University of Edinburgh, Edinburgh, UK

<sup>2</sup>NERC Radiocarbon Facility, East Kilbride, UK

<sup>3</sup>Biological and Environmental Sciences, University of Stirling, Stirling, UK

<sup>4</sup>Department of Biosciences, University of Durham, Durham, UK

<sup>5</sup>School of Environmental Sciences, University of Liverpool, Liverpool, UK

## Correspondence

Lorna E. Street, School of Geosciences, University of Edinburgh, Edinburgh EH9 3FF, UK.  
Email: lorna.street@ed.ac.uk

## Funding information

This work was supported by NERC grant NE/K000284/1 (P.A.W.) as part of the NERC Arctic Programme, and by a NERC fellowship grant to L.E.S. (NE/N015460/1).

## Abstract

Carbon cycle feedbacks from permafrost ecosystems are expected to accelerate global climate change. Shifts in vegetation productivity and composition in permafrost regions could influence soil organic carbon (SOC) turnover rates via rhizosphere (root zone) priming effects (RPEs), but these processes are not currently accounted for in model predictions. We use a radiocarbon (bomb-<sup>14</sup>C) approach to test for RPEs in two Arctic tall shrubs, alder (*Alnus viridis* (Chaix) DC.) and birch (*Betula glandulosa* Michx.), and in ericaceous heath tundra vegetation. We compare surface CO<sub>2</sub> efflux rates and <sup>14</sup>C content between intact vegetation and plots in which below-ground allocation of recent photosynthate was prevented by trenching and removal of above-ground biomass. We show, for the first time, that recent photosynthate drives mineralization of older (>50 years old) SOC under birch shrubs and ericaceous heath tundra. By contrast, we find no evidence of RPEs in soils under alder. This is the first direct evidence from permafrost systems that vegetation influences SOC turnover through below-ground C allocation. The vulnerability of SOC to decomposition in permafrost systems may therefore be directly linked to vegetation change, such that expansion of birch shrubs across the Arctic could increase decomposition of older SOC. Our results suggest that carbon cycle models that do not include RPEs risk underestimating the carbon cycle feedbacks associated with changing conditions in tundra regions.

## KEYWORDS

arctic, below-ground, isotopes, mycorrhiza, priming, radiocarbon, rhizosphere, root, shrub, vegetation change

## 1 | INTRODUCTION

Current estimates of net CO<sub>2</sub> release from permafrost ecosystems vary from around 20 billion to more than 200 billion tonnes of C by the end of this century (Gasser et al., 2018; Natali et al., 2019; Schuur et al., 2015; Turetsky et al., 2019). If C losses approach

~100 billion tonnes, this alone could exceed remaining emissions budgets for meeting the UN Paris Agreement 1.5°C target (Tokarska & Gillett, 2018). In the near term, increased plant productivity or 'greening' at high latitudes is expected to partially compensate for increased mineralization of soil organic carbon (SOC) in warming soils (Bjorkman et al., 2018; Burke, Chadburn,

This is an open access article under the terms of the Creative Commons Attribution License, which permits use, distribution and reproduction in any medium, provided the original work is properly cited.

© 2020 The Authors. *Global Change Biology* published by John Wiley & Sons Ltd

& Ekici, 2017; Elmendorf et al., 2012). In some tundra regions the abundance of tall woody shrubs is already increasing (Myers-Smith et al., 2011). However, the potential gains in C storage in plant biomass are small (1–3 kg C/m<sup>2</sup> if tall shrub tundra replaces sedge tundra; Berner, Jantz, Tape, & Goetz, 2018), compared to the large amount of C contained in surface soils (~10–100 kg/m<sup>2</sup> in the top 1 m; Hugelius et al., 2014). Changes in SOC storage in the active layer, the seasonally unfrozen part of the soil profile that lies above the perennially frozen permafrost, are expected to be as important as permafrost thaw in determining the strength of the permafrost C feedback (PCF) during the first half of the current century (Burke, Chadburn, et al., 2017). Carbon storage in the active layer will be determined by whether increasing C inputs outweigh C losses from faster SOC turnover. Reducing uncertainty around the PCF therefore relies on our understanding of how SOC mineralization rates will respond to changing environmental conditions, including vegetation change.

SOC mineralization rate depends on abiotic conditions such as temperature and moisture as well as the chemical characteristics of soil organic matter, but rates can also be influenced or 'primed' by the availability of labile C substrates (Blagodatskaya & Kuzyakov, 2008). Priming effects are defined as a change in the rate of mineralization of existing SOC in response to an added substrate. Priming responses to labile C are generally positive as high energy compounds stimulate the microbial decomposer community (Kuzyakov, Friedel, & Stahr, 2000). In Arctic soils, small additions of glucose increase the relative rate of CO<sub>2</sub> production from native SOC by ~30% in organic soils and by ~150% in mineral soils (Wild et al., 2014). Rhizosphere priming effects (RPEs)—the influence of living plant roots on SOC mineralization rates—are thought to arise via a similar mechanism, as root exudates and rhizodeposits provide high energy C substrates to soil microbes. RPEs also often have a positive effect on SOC mineralization, but not consistently so (Huo, Luo, & Cheng, 2017). RPEs are much more difficult to quantify than priming effects from experimental substrate additions because quantifying SOC mineralization in the presence of roots requires below-ground respiration to be partitioned into autotrophic and heterotrophic sources. This partitioning is difficult to achieve even under controlled conditions (Subke, Inglema, & Francesca Cotrufo, 2006), and as such, the evidence for the presence of in situ RPEs is limited (Huo et al., 2017). Key field-based evidence for RPEs is inferred from shifts in the natural abundance radiocarbon (<sup>14</sup>C) content of respired SOC in the presence of plants—these effects have been observed in Arctic mountain birch forest (Hartley et al., 2012) and in peatlands (Gavazov et al., 2018).

If mineralization of native SOC can be positively primed by below-ground inputs of labile plant C, there may be an important link between plant activity in permafrost systems and SOC turnover in the active layer. If SOC turnover increases with vegetation change, it would be possible for Arctic ecosystems to gain C through increasing plant biomass while losing C from the soil. There is some field data to support this—some more productive high latitude forest and shrub ecosystems have lower total soil C

than the nearby less productive tundra (Hartley et al., 2012; Parker, Subke, & Wookey, 2015; Sørensen et al., 2018; Wilmking, Harden, & Tape, 2006). However, current estimates of the PCF are largely based on models that represent SOC decomposition responses to temperature and moisture. These models do not take into account rhizosphere processes, which may influence the vulnerability of SOC to decomposition (Koven et al., 2015; Schädel et al., 2014). Earth system model predictions of the PCF are highly sensitive to how SOC mineralization processes are represented, so if current models are missing a key driver of SOC turnover, the impact on predicted climate feedbacks could be very significant (Burke, Chadburn, et al., 2017).

There is therefore an urgent need to understand the links between changes in vegetation distribution and productivity, and SOC turnover. In this study we ask: do RPEs influence SOC mineralization rates in permafrost ecosystems? If so, do RPEs differ between vegetation types, which may shift in abundance with Arctic greening? We develop the radiocarbon (bomb-<sup>14</sup>C) approach of Hartley et al. (2012) and Gavazov et al. (2018) to compare RPEs in two species of tall woody shrub vegetation versus ericaceous heath tundra, using a novel Bayesian mixing model approach to examine potential positive and negative RPEs. We test whether the allocation of recent photosynthate C (RPC) below-ground influences SOC mineralization by comparing the <sup>14</sup>C content of soil CO<sub>2</sub> effluxes with and without an intact plant canopy, using two-source mixing models: (a) a null model in which there are no priming effects and (b) a model in which either positive or negative RPEs can impact both the <sup>14</sup>C content of respired SOC and the rate of SOC mineralization.

We hypothesize that evidence for RPEs will be strongest in tall shrub tundra vegetation, which has greater above-ground biomass and is more productive than ericaceous heath tundra. Previous work at the same site (Street et al., 2018) has shown that a larger proportion of recent photosynthate is allocated below-ground in birch shrub vegetation compared to alder (a nitrogen fixing species). Recently fixed C in birch shrub vegetation is also widely distributed throughout the soil profile, while in alder recent photosynthate is mostly retained within plant root biomass (Street et al., 2018). We therefore expect RPEs to be greater in birch vegetation compared to alder because of greater labile C inputs to the soil under birch.

## 2 | MATERIALS AND METHODS

### 2.1 | Experimental design

We worked within Siksik creek catchment, a subcatchment of Trail Valley Creek in the uplands of the Mackenzie delta region, approximately 60 km north of Inuvik, NW Territories, Canada. The landscape is within the continuous permafrost zone and is characterized by rolling hills with a mean elevation of c. 100 m above sea level, and up to 30 m elevation change between valley bottom and hill top. Mean air temperatures in the region are –20.9°C from October to April, and 7.7°C from May to September (Teare, 1998).

Precipitation in 2014 was 277 mm, similar to the mean annual precipitation from 1960 to 2005 (Dean et al., 2016; Marsh, Onclin, & Neumann, 2002). Soils at the site are organic-rich turbic cryosols with an organic layer of approximately 0.05–0.5 m thickness, overlying a ~1 m thick Pleistocene till layer (Dean et al., 2016, 2018; Rampton, 1988).

We established three pairs of replicate 0.5 × 0.5 m plots in three vegetation types; (a) tall shrub vegetation dominated by alder (*Alnus viridis* (Chaix) DC.), (b) tall shrub vegetation dominated by birch (*Betula glandulosa* Michx.) and (c) dwarf shrub tundra predominantly composed of ericaceous species ('ericaceous heath tundra'). Plots were established on 18 August 2013, during the thaw season 1 year prior to sample collection (Table S1 provides information on understorey plant composition, soil thaw depth and organic layer depth for the experimental plots). To prevent below-ground allocation of RPC we removed all above-ground biomass from one of each pair of plots by cutting the stems at the ground surface, leaving the moss layer intact. The plant removal treatment was randomly allocated to one of each pair of plots. Each plot was also 'trenched' to a depth of 0.2 m by carefully cutting around the outside of the plot with a knife, in order to sever root connections in the surface organic layer. We observed a limited amount of shrub regrowth the following year, and this was removed before measurement. A 0.16 m diameter surface respiration collar was installed in the centre of each plot, and sealed to the ground surface with putty (Plumber's Mait, Evo-stick) to avoid severing roots or rhizomes in the intact plots. We monitored soil temperature in the intact and plant removal plots every 4 hr using iButton data loggers, and on 13 July 2014 sampled soils for determination of gravimetric soil water content (see Data S1).

## 2.2 | <sup>14</sup>C sample collection and analysis

We collected CO<sub>2</sub> samples for <sup>14</sup>C determination on three occasions; on 21–22 June, 10–13 July and 7–9 September 2014. CO<sub>2</sub> samples from the surface respiration collars were collected onto molecular sieve cartridges using an established technique (Hardie, Garnett, Fallick, Rowland, & Ostle, 2005), for more details see Data S2. Freezing weather conditions and strong winds meant we were unable to collect sufficient CO<sub>2</sub> for analysis from the heath tundra plots in September. To quantify the <sup>14</sup>C content of CO<sub>2</sub> respired at depth in the soil profile we inserted 6 mm diameter stainless steel probes to a depth of 0.2 m, approximately 0.2 m distant from each surface respiration collar. The probe inlet holes were sealed with a gas permeable, water-tight membrane (Street et al., 2016) and a molecular sieve cartridge was connected to the other end of the probe (Garnett & Hardie, 2009). At 0.2 m depth, all but two probes sampled CO<sub>2</sub> from mineral soil horizons. CO<sub>2</sub> was collected from the probes for a continuous period of 6 weeks beginning end of July 2014 (we were unable to collect enough CO<sub>2</sub> for analysis in one intact heath tundra plot). Molecular sieve cartridges were returned to

the NERC Radiocarbon Facility (East Kilbride), United Kingdom and the CO<sub>2</sub> recovered by heating and cryogenic purification (Garnett & Murray, 2013).

## 2.3 | Respiration measurements

We quantified surface CO<sub>2</sub> efflux rates immediately prior to collecting <sup>14</sup>CO<sub>2</sub> samples, using the same collars and an EGM-4 infrared gas analyzer (IRGA) connected to a CPY-4 plant canopy chamber (PP Systems). The chamber (2.4 L volume) was fully darkened prior to measurement using a custom-made light-proof cover. CO<sub>2</sub> concentrations in the chamber were recorded every 20 s over a 2 min period, and CO<sub>2</sub> fluxes were calculated based on the rate of change of CO<sub>2</sub> concentrations, using the linear term from a second-order polynomial fit in R (version 3.5.1).

## 2.4 | Soil profile <sup>14</sup>C sampling

We sampled three organic soil profiles in each vegetation type for <sup>14</sup>C determination. A trench was excavated exposing a vertical face from which 1 or 2 cm sections of approximately 16 cm<sup>2</sup> were cut using a knife. Care was taken to clean the knife thoroughly before removing each section in order to prevent contamination between layers. An initial profile was sampled in 2013, followed by two further profiles in 2014. Bulk soil samples were combusted in sealed quartz glass tubes and recovered as CO<sub>2</sub> following cryogenic purification.

## 2.5 | <sup>14</sup>C determination and interpretation

For all radiocarbon samples the recovered CO<sub>2</sub> was split into aliquots. One aliquot was converted to graphite via Fe–Zn reduction and measured for <sup>14</sup>C content using accelerator mass spectrometry at the Scottish Universities Environmental Research Centre (East Kilbride, UK). A second aliquot was used for determining δ<sup>13</sup>C (relative to the Vienna PDB international standard) by isotope ratio mass spectrometry (Thermo-Fisher Delta V). We used the δ<sup>13</sup>C values to correct the <sup>14</sup>C results for isotopic fractionation following convention, and expressed the <sup>14</sup>C data as %modern and conventional radiocarbon ages (in years BP, where 0 BP = AD 1950; Stuiver & Polach, 1977).

We also used the δ<sup>13</sup>C data to calculate the fractional component of atmospheric CO<sub>2</sub> ( $f_{\text{air}}$ ) in the respired CO<sub>2</sub> samples:

$$f_{\text{air}} = (\delta_s - \delta_r) / (\delta_a - \delta_r), \quad (1)$$

where  $\delta_s$ ,  $\delta_a$  and  $\delta_r$  are the δ<sup>13</sup>C values of the recovered sample (s), atmospheric CO<sub>2</sub> (a) and soil respiration in the absence of atmospheric CO<sub>2</sub> (r) respectively. We determined  $\delta_a$  from atmospheric CO<sub>2</sub> collected at the field site by drawing ambient air through a molecular

sieve cartridge, and  $\delta_i$  from  $\text{CO}_2$  recovered from soil incubations that excluded atmospheric  $\text{CO}_2$ .

The  $^{14}\text{C}$  content of respired  $\text{CO}_2$  ( $\Delta_r$ ) in the absence of atmospheric  $\text{CO}_2$  was then calculated using:

$$\Delta_r = (\Delta_s - f_{\text{air}} \times \Delta_a) / (1 - f_{\text{air}}), \quad (2)$$

where  $\Delta_s$  is the sampled  $^{14}\text{C}$  value from the surface collars,  $\Delta_a$  represents the  $^{14}\text{C}$  content of atmospheric  $\text{CO}_2$  at the field site during the year of sampling (collected using molecular sieve traps).

Nuclear weapons testing at the end of the 1950s to the mid-1960s enriched the atmosphere with  $^{14}\text{CO}_2$  resulting in a 'bomb-peak' in atmospheric  $^{14}\text{C}$  levels (Levin & Hesshaimer, 2016). Atmospheric  $^{14}\text{CO}_2$  has since decreased but remains elevated relative to when nuclear testing began. The theoretical atmospheric  $^{14}\text{CO}_2$  content in 1950 is defined as 100 %modern - C fixed from the atmosphere prior to 1950 ("pre-bomb") has a  $^{14}\text{C}$  content < 100 %modern and will generally be older the lower the %modern value (as a result of radioactive decay).

## 2.6 | Statistical analysis

To test for differences in the  $^{14}\text{C}$  content of soil  $\text{CO}_2$  efflux between vegetation types and treatments, we fit mixed effects linear models using the nlme package (version 3.1-137) for R (version 3.5.1).  $^{14}\text{C}$  data for the tundra heath vegetation in September were missing, so we analysed the data twice using (a) only the birch and alder shrub data, so every time point plus interactions could be included in the full model and (b) using only the June and July time points, so all vegetation types and interactions could be included. We incorporated vegetation type, treatment and measurement date as fixed effects, and plot as a random effect to account for the repeated measures design. We did not include a random effect to account for the plot pairing as this did not explain any additional variation in the models that is, the soils were too spatially variable for the pairing to be effective. We also included a variance function (using weights = varIdent) in the model to account for heterogeneity of variances between groups (Pinheiro & Bates, 2009). In all cases, three-way interaction terms with measurement date were insignificant and, based on likelihood ratio tests, did not provide an improvement in model fit, so were removed.

To test for differences in soil  $\text{CO}_2$  efflux ( $F_s$ ) between vegetation types and treatments, we also fitted mixed effects linear models. However, because in September we estimated relative  $F_s$  fluxes between treatments based on the amount of  $\text{CO}_2$  build-up in the  $^{14}\text{C}$  sampling chambers (ppm/min), rather than measuring flux rates with the IRGA, we excluded the September data. There was no missing respiration data from the June and July time points, so we incorporated vegetation type, treatment and measurement date (June or July) as fixed effects, and plot as a random effect. We also included a variance function (using weights = varIdent()) in the model to account for heterogeneity of variances between groups (Pinheiro & Bates, 2009). The

three-way interaction term between vegetation type, treatment and measurement date was insignificant and did not improve model fit, so was removed.

We tested the effect of the plant removal treatment on the  $^{14}\text{C}$  content and concentration of pore space  $\text{CO}_2$  at 0.2 m depth by fitting generalized least squares models, with vegetation type and treatment as factors (nlme package for R version 3.5.1). Variance functions were included to account for heterogeneity of variances between treatments.

## 2.7 | Mixing model analysis

To test for priming effects of RPC on heterotrophic respiration we carried out two separate analyses, both based upon two-source mixing models. In the first analysis we assume there are no priming effects (the 'null model') and test whether a simple two-source mixing model can simulate the  $^{14}\text{C}$  content of soil  $\text{CO}_2$  efflux in the intact plots, given the observed data and errors (Equation 3a,b, Figure 1a):

$$\Delta_{r-\text{intact}} = (\Delta_{r-\text{het}} \times [1 - f_{\text{RPC}}]) + (\Delta_{\text{RPC}} \times f_{\text{RPC}}), \quad (3a)$$

where

$$f_{\text{RPC}} = 1 - \left( \frac{F_{S,\text{removal}}}{F_{S,\text{intact}}} \right). \quad (3b)$$

$\Delta_{r-\text{intact}}$  and  $\Delta_{r-\text{het}}$  are the  $^{14}\text{C}$  content of soil  $\text{CO}_2$  efflux from the intact plots and plant removal plots,  $\Delta_{\text{RPC}}$  is the  $^{14}\text{C}$  content of RPC,  $f_{\text{RPC}}$  is the fraction of soil  $\text{CO}_2$  efflux derived from RPC,  $F_{S,\text{intact}}$  and  $F_{S,\text{removal}}$  are the surface  $\text{CO}_2$  efflux rates in intact and plant removal plots. This model assumes that both the absolute flux rate, and the  $^{14}\text{C}$  content, of soil  $\text{CO}_2$  efflux from the plant removal plots reflect the rate and  $^{14}\text{C}$  content of heterotrophic respiration in the intact plots. In this case, the measured difference in  $F_s$  between treatments reflects the contribution of RPC to respiration in the intact plots (Equation 3b), and a two source mixing model should be able to reproduce the observed  $^{14}\text{C}$  content of soil  $\text{CO}_2$  efflux in the intact plots (Figure 1a, Equation 3a). There is likely to be some residual respiration from live roots in the plant removal plots, but we assume this is small and include it implicitly as part of the heterotrophic fraction.

We accounted for error in the observations by representing the isotopic end-members ( $\Delta_{r-\text{het}}$  and  $\Delta_{\text{RPC}}$  in Equation 3a) and the mixing fraction for RPC ( $f_{\text{RPC}}$ ) as normal distributions, based on the mean and standard deviation (SD) of the observed values. For  $\Delta_{r-\text{het}}$  we used the mean and SD of the measured  $^{14}\text{C}$  content of  $\text{CO}_2$  flux from the plant removal plots. For the fraction of respiration from RPC ( $f_{\text{RPC}}$ ), we used the mean and SD of the relative soil  $\text{CO}_2$  efflux rates in the intact and plant removal treatments, truncating the normal distribution between 0 and 1 to ensure all terms in the mixing model are positive. For the  $^{14}\text{C}$  content of RPC we used an estimated value of atmospheric  $^{14}\text{CO}_2$  for 2014, based on the measured value in 2015

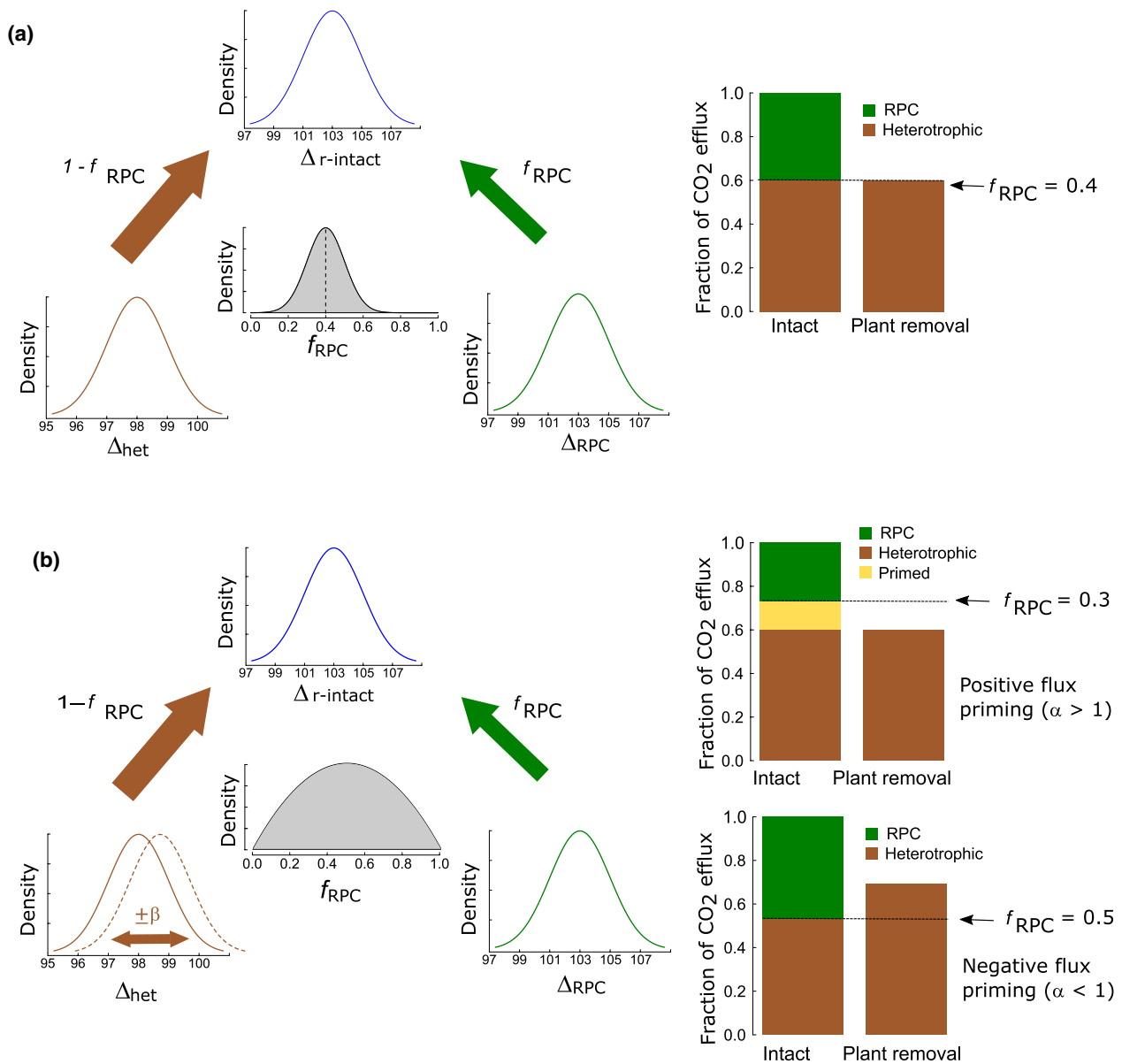


**FIGURE 1** Schematic representation of two-source mixing models with and without priming effects. (a) Two-source mixing model without priming effects (the null model). This model assumes that the difference in soil CO<sub>2</sub> effluxes between intact and plant removal plots reflects the contribution of recent photosynthate-derived C ( $f_{RPC}$ , here  $f_{RPC} = 0.4$ ). In the null model analysis, we simulate the distribution of expected values for soil efflux <sup>14</sup>CO<sub>2</sub> in the intact plots, based on the observed differences in soil CO<sub>2</sub> efflux rates and <sup>14</sup>CO<sub>2</sub> from the plant removal treatment, including observed errors. We compare the simulated distributions to soil efflux <sup>14</sup>CO<sub>2</sub> data from the intact plots to test whether the null model is consistent with the observed values; (b) two-source mixing model with priming effects. This model does not assume that the difference in soil CO<sub>2</sub> efflux rates between intact and plant removal plots reflects the proportional contributions of recent photosynthate carbon ( $f_{RPC}$ ) and heterotrophic respiration—rhizosphere priming effects can potentially result in either a stimulation (positive priming) or a suppression (negative priming) of heterotrophic respiration rates. In this analysis, we optimize the model to fit the observed values of soil CO<sub>2</sub> efflux <sup>14</sup>CO<sub>2</sub> in intact plots, to produce joint distributions for  $\alpha$  and  $\beta$  that are consistent with the observed data, while  $f_{RPC}$  is free to vary between 0 and 1

minus 0.4%modern  $\pm$  AMS analytical error ( $103.87 \pm 0.49\%$ modern). Using a mean <sup>14</sup>CO<sub>2</sub> value that assumes plant photosynthate is on average 0.5%modern more enriched, or 0.5%modern less enriched, does not change our results (Data S3; Figure S4). We then simulate the expected <sup>14</sup>C content of soil CO<sub>2</sub> efflux in the intact plots by generating 100,000 random samples from these distributions. If the observed mean <sup>14</sup>CO<sub>2</sub> for the intact plots falls outside the 95% highest density interval (hdi) of the simulated mean, we conclude

that the null model is insufficient to explain the observations given the associated error—and therefore that the observed data provide evidence of priming.

We carried out a second model analysis for the peak growing season data, in which we assume possible plant removal effects on heterotrophic respiration (Figure 1b, Equation 4a,b):

$$\Delta_{r-intact} = ([\Delta_{r-het} + \beta] \times [1 - f_{RPC}]) + (\Delta_{RPC} \times f_{RPC}), \quad (4a)$$

where

$$f_{\text{RPC}} = 1 - \left( \alpha \times \frac{F_{\text{S,removal}}}{F_{\text{S,intact}}} \right). \quad (4b)$$

$\Delta_{\text{r-intact}}$  and  $\Delta_{\text{r-het}}$  are the  $^{14}\text{C}$  content of soil  $\text{CO}_2$  efflux from the intact plots and plant removal plots,  $\Delta_{\text{RPC}}$  is the  $^{14}\text{C}$  content of RPC,  $f_{\text{RPC}}$  is the fraction of soil  $\text{CO}_2$  efflux derived from RPC,  $F_{\text{S,intact}}$  and  $F_{\text{S,removal}}$  are the surface  $\text{CO}_2$  efflux rates in intact and plant removal plots,  $\alpha$  is a parameter representing priming effects on the flux rate of heterotrophic respiration,  $\beta$  and is a parameter representing a shift in the  $^{14}\text{C}$  content of the heterotrophic respiration C source.

The priming model allows for impacts of RPC on both the rate (which we refer to as a 'flux rate change', parameter  $\alpha$ ) and the  $^{14}\text{C}$  content (a 'source-shift', parameter  $\beta$ ) of heterotrophic respiration in intact vegetation. If there is no heterotrophic flux rate-change in response to plant removal, the difference in  $F_{\text{S}}$  between treatments will reflect the contribution of RPC to  $F_{\text{S}}$  in the intact plots. However, if priming effects on heterotrophic respiration rates are present we cannot assume this to be the case, and so cannot estimate the RPC contribution to soil  $\text{CO}_2$  efflux by comparing  $F_{\text{S}}$  between treatments. We therefore allowed the fraction of  $f_{\text{RPC}}$  to be unconstrained between 0 and 1, and estimate the joint distribution for potential flux rate changes and  $^{14}\text{C}$  source-shifts that satisfies isotopic mass balance in the mixing model and is consistent with the observed data. This analysis was carried out with the RStan package (version 2.18.2) for R version 3.5.1. We provide more information on model assumptions and our choice of priors in Data S3.

### 3 | RESULTS

#### 3.1 | Treatment effects on soil $\text{CO}_2$ efflux and $^{14}\text{C}$

We removed above-ground vascular plant biomass from treatment plots to prevent below-ground allocation of RPC. This resulted in a reduction in soil  $\text{CO}_2$  efflux rate ( $F_{\text{S}}$ ) in the plant removal plots (Figure 2a; Figure S3; Table S2) but the relative difference in  $F_{\text{S}}$  between intact and plant removal plots decreased as the thaw season progressed (Figure 2a; Table S2). There was a large increase in absolute soil  $\text{CO}_2$  efflux rates in both treatments between June and July (Figure S3). The average radiocarbon content of soil  $\text{CO}_2$  efflux was either equal to, or more depleted than, ambient atmospheric  $^{14}\text{CO}_2$  for all sampling times and treatments (Figure 2b,c). We found no significant differences in the  $^{14}\text{C}$  content of  $\text{CO}_2$  efflux between treatments in any vegetation type (Table S3), but soil  $\text{CO}_2$  efflux under birch shrubs was consistently enriched in  $^{14}\text{C}$  (by  $\sim 1.3\%$  modern) relative to alder across all sampling periods (linear mixed effects model,  $n = 3$ ,  $p = .02$ ) and also tended to be more enriched relative to both alder and heath tundra vegetation in June and July only (linear mixed effects model,  $n = 3$ ,  $p = .1$ ).

We found no significant treatment effects on soil temperature or moisture (Figures S1b and S2) and no relationship between surface

efflux  $^{14}\text{C}$  and temperature (Figure S2). In June the average thaw depth in alder was 0.1 m and in heath tundra 0.27 m, with birch intermediate. By July, thaw depths had increased to c. 0.3 m in alder, and c. 0.5 m in both the other vegetation types. There was no effect of treatment on thaw depth (Table S1).

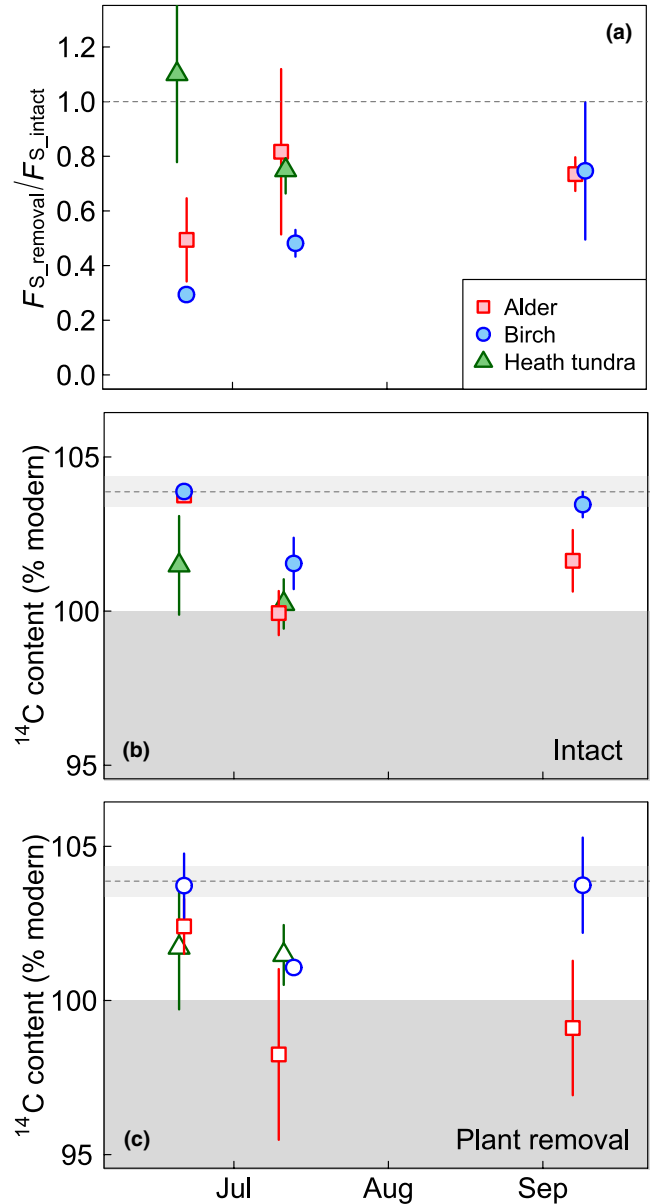


**FIGURE 2** Impacts of plant removal treatment on soil  $\text{CO}_2$  efflux rates and  $^{14}\text{C}$  content. (a) Soil  $\text{CO}_2$  efflux rates in the plant removal plots as a fraction of soil  $\text{CO}_2$  efflux in the intact plots for alder shrub, birch shrub and heath tundra vegetation ( $n = 3$ ), (b)  $^{14}\text{C}$  content of soil  $\text{CO}_2$  efflux in intact plots ( $n = 3$ ), and (c) plant removal plots ( $n = 3$ ). Error bars are standard errors. The dashed line in (b) and (c) is the estimated atmospheric  $^{14}\text{CO}_2$  for 2014  $\pm 1\sigma$ . The shaded area represents 'pre-bomb'  $^{14}\text{C}$  values.  $^{14}\text{CO}_2$  in birch was significantly enriched by  $\sim 1.3\%$  modern compared to alder and heath tundra vegetation (Table S3a,b). There was no significant effect of plant removal treatment on the  $^{14}\text{C}$  content of soil  $\text{CO}_2$  efflux for any vegetation type

### 3.2 | In situ evidence for RPEs

A two-source mixing model with no priming effects (the 'null' model [Figure 1a]) was able to reproduce the  $^{14}\text{C}$  content of soil  $\text{CO}_2$  effluxes from intact plots for all vegetation types in June and September (Figure 3a–c,g,h). During the peak growing season in July, however, the null model overestimated the  $^{14}\text{C}$  enrichment of soil  $\text{CO}_2$  efflux in intact birch plots (Figure 3e). This is evident that either the rate and/or the  $^{14}\text{C}$  content of heterotrophically respired C changed in response to plant removal. The null model also overestimated the  $^{14}\text{C}$  enrichment of soil  $\text{CO}_2$  fluxes in heath tundra in July, but the observed mean value falls within the 95% hdi of the simulated mean value (Figure 3f). For alder, the null model was consistent with the observed  $^{14}\text{CO}_2$  data across all time points.

### 3.3 | Heterotrophic respiration is more $^{14}\text{C}$ -depleted in the presence of recently photosynthesized carbon

To estimate potential  $^{14}\text{C}$  shifts in the C source for heterotrophic respiration during July, we optimized a two-source mixing model

including RPEs (the 'priming' model [Figure 1b]) to the observed  $^{14}\text{CO}_2$  data. If RPEs are present, differences in  $F_s$  between intact and plant removal plots will reflect differences in heterotrophic respiration rates between treatments, in addition to the direct effect of reducing the autotrophic component of the flux. To account for this we assume no prior information on the partitioning between autotrophic versus heterotrophic  $\text{CO}_2$  sources—the fraction of  $f_{\text{RPC}}$  is allowed to vary between 0 and 1. It should be noted though, that because  $f_{\text{RPC}}$  cannot be less than zero, there is an upper limit to the value that  $\alpha$  can take (Figure 4). This value is smallest for alder at 1.25 and greatest for birch at 2.1.

In alder, a  $^{14}\text{C}$  shift was not required to reproduce the measured surface efflux  $^{14}\text{C}$  values (Figure 4a,d), consistent with the lack of evidence for priming in the null model analysis. During peak growing season, however, modelled heterotrophic respiration in intact birch vegetation is more depleted in  $^{14}\text{C}$  than in the plant removal treatment (Figure 4b,e). This negative shift in  $^{14}\text{C}$  content is apparent regardless of whether or not absolute rates of heterotrophic respiration increase (a positive rate change,  $\alpha > 1$ ) or decrease (a negative rate change,  $\alpha < 1$ ) in response to plant removal. However, the shift in heterotrophic  $^{14}\text{C}$  required to reproduce the observed

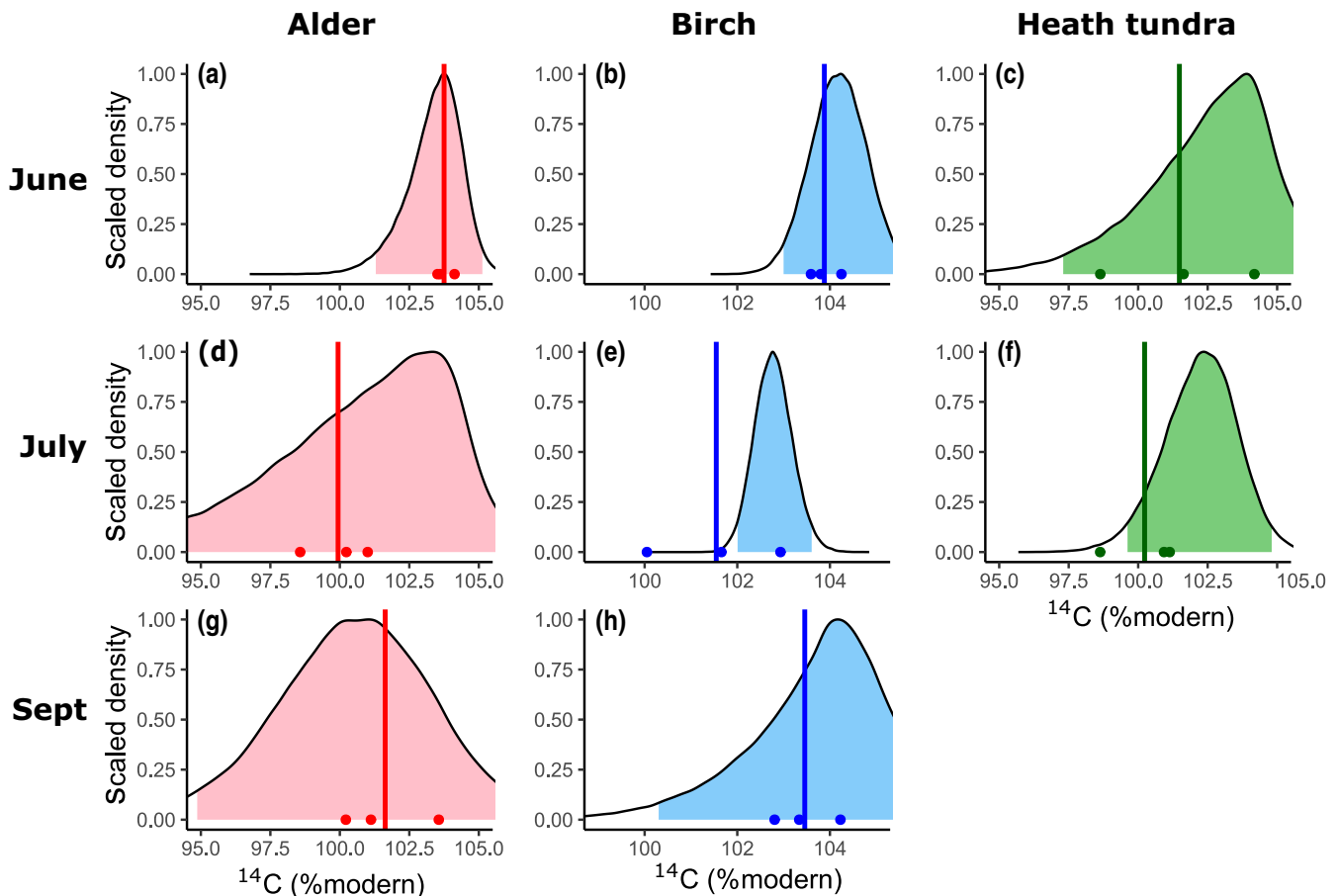


**FIGURE 3** (a–h) Simulated  $^{14}\text{C}$  content of soil  $\text{CO}_2$  efflux in intact vegetation using a two-source mixing model that assumes no priming effects (Equation 3a). Points are observed  $^{14}\text{CO}_2$  values ( $n = 3$ ), vertical lines are the mean of the observed values. Shaded areas are 95% highest probability density intervals for the simulated value. The mixing model overestimates the  $^{14}\text{C}$  content of soil  $\text{CO}_2$  efflux during peak growing season for birch and heath tundra (panels e and f).

efflux  $^{14}\text{CO}_2$  decreases as  $\alpha$  increases, and above  $\alpha \approx 1.6$  no shift in  $^{14}\text{C}$  is required to explain the observed values (Figure 4b). There is evidence of a similar negative shift in  $^{14}\text{C}$  in the heath tundra vegetation (Figure 4c), but in this case the average  $^{14}\text{C}$  shift is negative for all values of  $\alpha$ . For illustration purposes, if we assume that any heterotrophic flux rate change, which occurs as a result of RPEs, is likely to be positive but modest that is,  $+30\%$  ( $1 < \alpha < 1.3$ ), the most likely value for the shift in  $^{14}\text{C}$  content of heterotrophic respiration is c.  $0\%$  modern for alder shrub vegetation, c.  $-1.5\%$  modern for birch shrub vegetation and c.  $-2.1\%$  modern for heath tundra (Figure 4d–f).

### 3.4 | Evidence for the influence of recent photosynthate at 0.2 m

Average soil pore space  $^{14}\text{CO}_2$  in intact plots was depleted relative to ambient atmospheric values for all vegetation types and  $>100\%$  modern only in birch plots (Figure 5a). Pore space  $^{14}\text{CO}_2$  was significantly more enriched in the intact plots than in the plant removal plots overall (generalized least squares,  $p = .003$ , Figure 5a) driven by large differences between treatments in the shrub plots. Pore space  $^{14}\text{CO}_2$  was similar between treatments in the heath tundra. In the plant removal plots  $^{14}\text{CO}_2$  collected at 0.2 m was  $<100\%$  modern on average in all vegetation types (Figure 5a; Table S5). Soil pore  $\text{CO}_2$  concentrations at 0.2 m depth were also significantly lower in the plant removal plots (generalized least squares,  $p = .003$ , Figure 5b; Table S4).

### 3.5 | Radiocarbon content of organic soils

The maximum depth of the organic horizon in soil profiles sampled for their radiocarbon content varied from 0.12 to 0.24 m in alder, 0.03 to 0.1 m in birch and 0.12 to 0.20 m in heath tundra (Figure 6).  $^{14}\text{C}$  depth profiles under each vegetation type show that bulk soil  $^{14}\text{C}$  was  $<100\%$  modern at depths greater than  $\sim 0.1$  m in alder and birch vegetation, and at depths greater than  $\sim 0.05$  m in heath tundra (Figure 6). At 0.2 m depth bulk SOC beneath alder and heath tundra vegetation had conventional radiocarbon ages of  $\sim 600$  and 1,500 years respectively (Figure 6).

## 4 | DISCUSSION

### 4.1 | Plant removal decreased soil $\text{CO}_2$ efflux without significantly changing the $^{14}\text{C}$ content

The plant removal treatment had a clear impact on soil  $\text{CO}_2$  efflux rates, which were reduced by up to 70% in the treated plots. In June, and early September, rates of photosynthesis in the intact plots would have been lower than in July—measurements in June were made just after bud-burst and before shrub leaves had expanded, and in September after leaf senescence. We nevertheless saw clear differences in soil  $\text{CO}_2$  efflux rates between treatments, suggesting that roots in the intact plots were active and

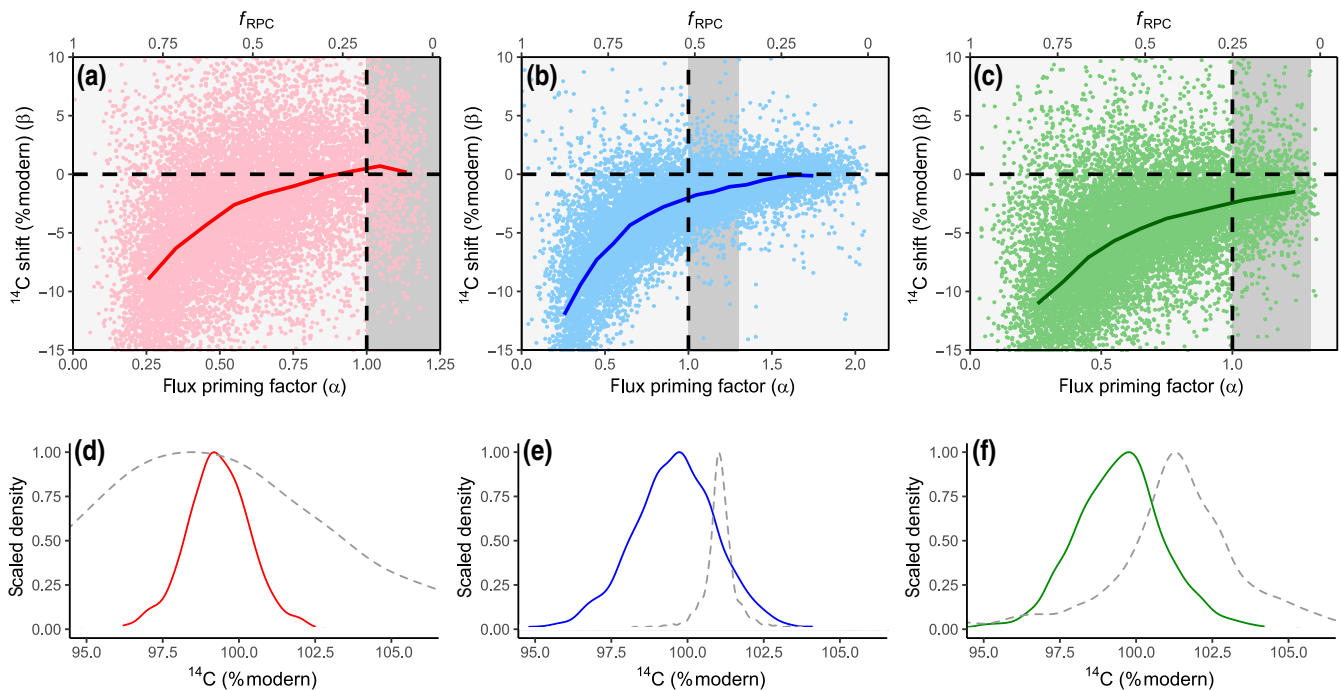


**FIGURE 4** Modelled priming effects on heterotrophic respiration fluxes and  $^{14}\text{C}$  content using a two-source mixing model (Equation 3b). (a–c) Posterior joint probability distributions for the  $^{14}\text{C}$  source-shift in heterotrophic respiration ( $\beta$ ) and the priming of heterotrophic flux rates ( $\alpha$ ). The solid line shows the median  $^{14}\text{C}$  shift which is consistent with the data, as priming of heterotrophic flux rates varies. The fraction of RPC derived respiration is allowed to vary in the model between 0 and 1. (d–f) Posterior probability distributions for the mean  $^{14}\text{C}$  content of heterotrophic respiration in intact (solid lines) and plant removal (grey dashed lines) plots, assuming modest positive priming of respiration flux rates ( $1 < \alpha < 1.3$ ; dark grey shaded areas in top row panels)



respiring at all sampling times. The relative difference in soil CO<sub>2</sub> efflux between treatments tended to decrease over time however, particularly in the tall shrub plots between June and July. This pattern is likely driven by large increases in absolute heterotrophic respiration rates as soils in both treatments warmed and thawed (Mikan, Schimel, & Doyle, 2002). Despite clear treatment effects on the absolute rates of soil CO<sub>2</sub> efflux, we saw little impact of the treatment on the <sup>14</sup>C content of CO<sub>2</sub>. In the absence of priming, we would expect the <sup>14</sup>C content of soil CO<sub>2</sub> efflux in the removal plots to be more depleted than the intact plots, because the RPC CO<sub>2</sub> source is relatively enriched in <sup>14</sup>C. Our mixing model analysis

was designed to explore the reasons for the lack of treatment effect, taking into account uncertainty in both the soil CO<sub>2</sub> efflux and <sup>14</sup>C data.

#### 4.2 | RPEs influence SOC mineralization in permafrost ecosystems

We find evidence for RPEs in peak growing season in birch vegetation, and weaker evidence in ericaceous heath tundra—the observed lack of treatment effect on the <sup>14</sup>C content of soil CO<sub>2</sub>

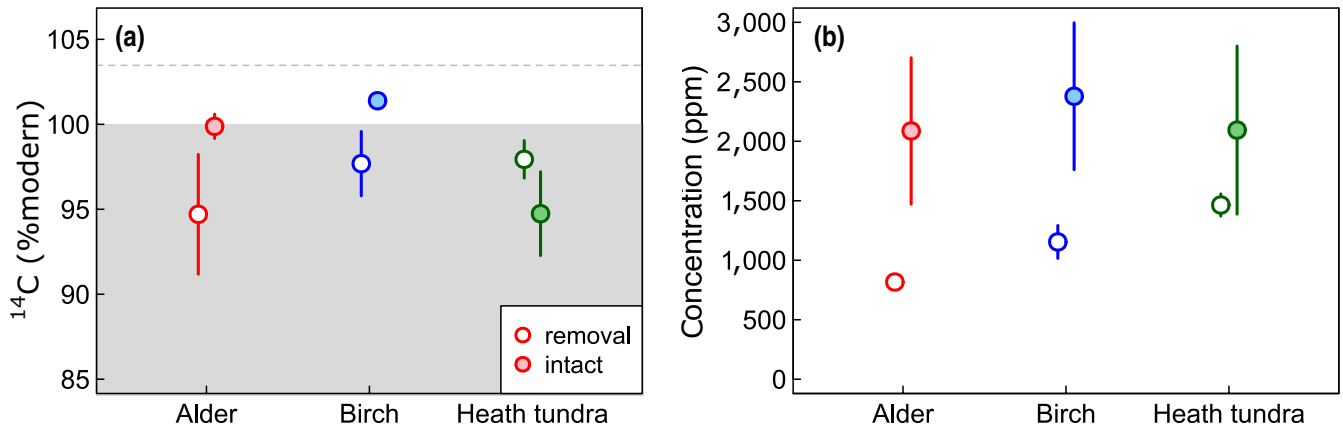


**FIGURE 5** Effects of plant removal on soil pore space CO<sub>2</sub> concentrations and <sup>14</sup>C at 0.2 m depth. (a) Pore space <sup>14</sup>CO<sub>2</sub> content and (b) CO<sub>2</sub> concentration at 0.2 m depth July–August 2014. Error bars are SE,  $n = 3$  except for Heath tundra intact plots where  $n = 2$ . The grey shaded area indicates pre-bomb <sup>14</sup>C values (less than 100%modern)

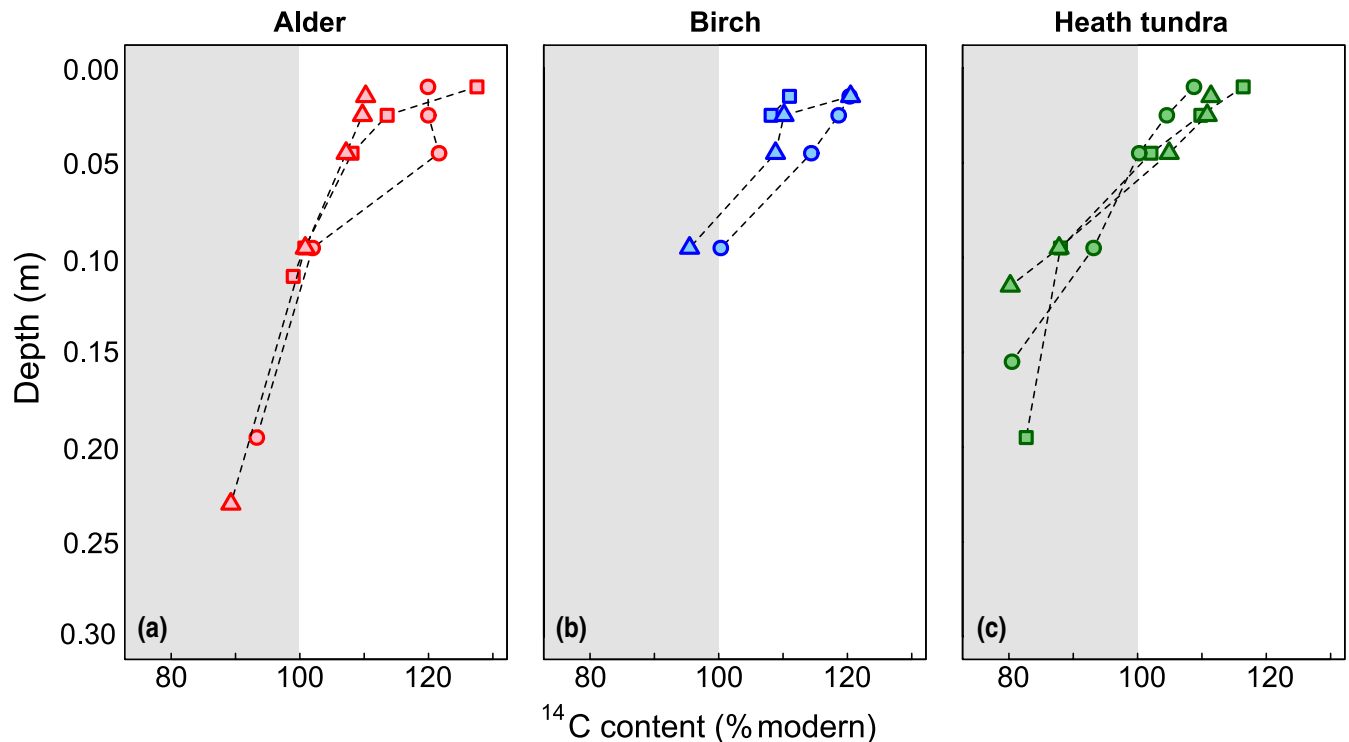


**FIGURE 6** Depth profiles for soil <sup>14</sup>C content. Bulk soil <sup>14</sup>C for organic soil horizons under (a) alder shrub (b) birch shrub and (c) heath tundra vegetation. Points represent individual data values for three soil profiles

efflux cannot be explained without inferring a change in either the rate of flux, or the  $^{14}\text{C}$  content, of heterotrophic respiration in the presence of an intact plant canopy. We find no evidence of RPEs in alder vegetation, or in any vegetation type outside the peak growing season. A lack of evidence does not mean we can conclusively say RPEs are not operating, as they may be present but undetectable. However, a lack of RPEs in spring and autumn would be consistent with controlled experimental studies which show that the strength of RPE responses are more closely related to plant leaf biomass—and therefore photosynthetic capacity—than root biomass (Huo et al., 2017). Other field studies have found seasonal patterns in RPEs in mountain birch forest (Hartley et al., 2012) but not in alpine peatlands (Gavazov et al., 2018). In our study, the observed responses to canopy removal, and the seasonal patterns, are consistent with a direct link between plant photosynthetic activity and SOC turnover, with the exception of alder-dominated vegetation.

As we expected, evidence for RPEs in birch shrub vegetation was stronger than in alder vegetation. Patterns of ecosystem carbon allocation in alder differ from those in birch, even though total canopy leaf nitrogen, and therefore photosynthetic capacity (Shaver et al., 2013), is similar between the two vegetation types at this location (Street et al., 2018). In birch vegetation, almost 30% of gross photosynthesis is delivered to bulk soils, either as root exudates or via plant-associated microbes, within 20 days of fixation; but in alder, which is an N-fixing plant (Mitchell & Ruess, 2009), the transfer of recent photosynthate to soils is low (Street et al., 2018). These differences in C allocation are likely linked to plant N acquisition: extensive ectomycorrhizal networks under birch (Deslippe & Simard, 2011) require below-ground C allocation to support uptake of N from soils (Hobbie & Hobbie, 2006). Carbon allocated below-ground in alder vegetation, however, is mostly retained within root tissues and nodules (Street et al., 2018) and is therefore not available to stimulate microbial decomposition in the soil. Less allocation of labile C below-ground may explain why we failed to detect priming under alder, and if so, this shows that patterns of plant allocation, as well as rates of photosynthesis, are important in driving priming responses. The lack of evidence for priming in alder is also consistent with the theory that RPEs arise because plants release labile C to directly stimulate microbial N release from soil organic matter, the so-called N-mining hypothesis (Dijkstra, Bader, Johnson & Cheng, 2009). Under this hypothesis, N-fixing plants would not be expected to drive RPEs because they can acquire N directly from the atmosphere, rather than relying on SOM turnover.

### 4.3 | Quantifying shifts in the $^{14}\text{C}$ of respired SOC

As we show here, the interactions between autotrophic and heterotrophic organisms in soils can change the isotopic composition of heterotrophic respiration, making it impossible to quantify the

isotopic end members in a two source mixing model. We deal with this problem by quantifying the region of joint parameter space for  $\alpha$  (the absolute rate of heterotrophic respiration) and  $\beta$  (the shift in isotopic composition of heterotrophic respiration) that is consistent with isotopic mass balance; we present a range of feasible solutions, rather than a single solution. Our analysis shows that as the parameter  $\alpha$  increases, the parameter  $\beta$  decreases. This means that the  $^{14}\text{C}$  shift in heterotrophically respired C required to explain the  $^{14}\text{C}$  content of soil  $\text{CO}_2$  effluxes in the intact plots is smaller under a positive priming scenario, compared to a negative priming scenario. For example, in birch vegetation, above  $\alpha \approx 1.6$  no shift in the  $^{14}\text{C}$  content of heterotrophically respired  $\text{CO}_2$  is required to explain the data. (An  $\alpha$  value of 1.6 would correspond to an increase in heterotrophic respiration from c.  $2 \mu\text{mol m}^{-2} \text{s}^{-1}$  to c.  $3.2 \mu\text{mol m}^{-2} \text{s}^{-1}$ .) This analysis shows that while both positive RPEs and negative RPEs are consistent with our observations and the isotopic mass balance model, the greater the negative RPE, the more extreme the  $^{14}\text{C}$  source-shift required to explain the data.

If we restrict the feasible solutions such that RPEs are positive, which they appear to be in most studies (Huo et al., 2017), up to a maximum value of 30% as recorded for Arctic soils under laboratory conditions (Wild et al., 2016), then predicted heterotrophic  $^{14}\text{CO}_2$  is c. 1.5% modern lower in the intact birch plots compared to the plant removal treatment. Because observed values of soil efflux  $^{14}\text{CO}_2$  in July were below atmospheric values, the only way the  $^{14}\text{CO}_2$  of the heterotrophic component can decrease is if there is a greater contribution from 'pre-bomb' (<100% modern) SOC. Carbon sources that are <100% modern were fixed from the atmosphere before the 'bomb-peak' of the 1950s and mid 1960s (Dean et al., 2018; Levin & Heshshaimer, 2016). We can be confident, therefore, that the SOC respired in the presence of RPC in birch vegetation is older because of a greater proportional contribution of C that is at least 50 years old.

We argue that the most parsimonious explanation for the heterotrophic  $^{14}\text{C}$  shift is a stimulation of SOC respiration at soil depths below the 'bomb-peak'—the depth at which bulk soil  $^{14}\text{C}$  contents are <100% modern. In Birch vegetation this occurs at c. 0.1 m, roughly at the transition between organic and mineral soil horizons. The implication that the RPEs we observe are driven by priming below 0.1 m is consistent with studies that show stronger priming responses in mineral horizons compared to surface organic layers in Arctic systems (Wild et al., 2014, 2016). This conclusion is also supported by the differences we see in  $\text{CO}_2$  concentration and  $^{14}\text{C}$  content at 0.2 m depth, both of which indicate the presence of RPC derived  $\text{CO}_2$  at 0.2 m in the intact plots, even though rooting density declines below c. 0.15 m in these systems (Street et al., 2018). In heath tundra organic horizons are also c. 0.1 m but the depth at which bulk soil  $^{14}\text{C}$  contents are <100% modern is shallower at 0.05 m. In this case, either organic or mineral soils could have provided a source of <100% modern C. The fact that RPEs appear to be operating at, or below, the limit of the surface organic horizon contrasts with the results of Hartley et al. (2012), who infer priming of mainly post-bomb SOC in the surface ~0.02 m of mountain birch soils.

Soil organic horizons under birch were generally shallower than in alder and ericaceous heath tundra, and as such contained a smaller total amount of pre-bomb SOC. The fact that we found less pre-bomb SOC in birch organic horizons is consistent with the observed  $^{14}\text{CO}_2$  of surface effluxes, and the  $^{14}\text{C}$  of  $\text{CO}_2$  produced at 0.2 m depth, both of which show respired  $\text{CO}_2$  tended to be more enriched in  $^{14}\text{C}$  under birch. Taken together, our results suggest that older (>50 years old) SOC is less abundant in birch organic soil and this may result directly from positive RPEs in birch vegetation.

#### 4.4 | Mitigation of experimental artefacts

Our approach of removing above-ground biomass to eliminate below-ground RPC inputs could have led to experimental artefacts if root mortality increased. Root mortality could have led to an increase in plant-derived C inputs in the form of root litter (and mycorrhizal fungal biomass), potentially causing priming effects. We minimized the likelihood of this 'root death priming' by removing the above-ground biomass 1 year prior to sampling, such that any pulse of labile C from the death of ephemeral fine-roots or fungal biomass peaked the previous season (Högberg et al., 2001). In any event, the data show that the effect of root death must have been small by the time we sampled in 2014—if plant C inputs from root death were driving significant priming effects, we would expect to see evidence of this in June and September, but we saw no evidence of priming at these times.

The plant removal treatment could also have resulted in experimental artefacts if there was an impact on soil abiotic conditions; reduced shading could potentially increase soil temperatures or cause soil drying, or conversely reduced transpiration rates could increase soil moisture content. Our expectation was that these effects would be small because (a) the moss layer has a strong impact on soil water and energy fluxes in these systems (Blok et al., 2011) and we left the moss layer intact, (b) the plots were on gently sloping ground so reduced transpiration would be unlikely to influence soil moisture at depth where these permafrost soils are generally saturated (Street et al., 2016) and (c) the plots were small and sun angles at the study location are low so plots would still be shaded to a large extent by the surrounding vegetation. Above-ground plant removal will have influenced abiotic conditions to a degree, but we found no evidence of a treatment effect on soil temperatures or soil moisture in surface soils (Figure S1), nor did we find a relationship between soil  $\text{CO}_2$  efflux  $^{14}\text{C}$  content and surface temperatures (Figure S2). We are confident therefore that reduced below-ground C allocation, rather than abiotic factors, is the most likely explanation for the priming effects we observe.

We saw clear differences between treatments in the  $^{14}\text{C}$  content of  $\text{CO}_2$  at 0.2 m depth, but no differences in the  $^{14}\text{C}$  content of the surface  $\text{CO}_2$  efflux.  $\text{CO}_2$  production rates are likely to be lower at depth than in the surface organic horizons, and we would also expect the diffusivity of  $\text{CO}_2$  in mineral soils at 0.2 m to be much lower than in the more porous overlying organic layer. It is likely then, that  $\text{CO}_2$  from 0.2 m depth makes only a small contribution to the surface

$\text{CO}_2$  efflux, and the differences in  $^{14}\text{C}$  content we measured at depth are masked by  $\text{CO}_2$  production from organic soil in shallower layers.

#### 4.5 | Implications

Our results have significant implications for how SOC decomposition is represented in ESMs that include the permafrost carbon cycle feedback (PCF): (a) Decomposition of SOC which is >50 year old can be influenced by the presence of recent photosynthate, so model parameterizations based on long-term laboratory incubation data in the absence of plants likely underestimate the 'inherent vulnerability' of SOC to decomposition. (b) We show that RPEs influence how decomposition rates vary with soil depth, likely increasing decomposition below the zone of maximum root density. The extent to which SOC turnover varies with depth in the active layer is a major if not the most important uncertainty in current ESMs predictions of the PCF (Burke, Ekici, et al., 2017), so it will be important to account for rhizosphere priming mechanisms in large-scale C models going forward. (c) RPEs may not be associated with higher plant productivity if plant C allocation below-ground is limited—therefore, plant C allocation patterns are relevant to understanding how SOC turnover will respond to changing vegetation under predicted climate change in permafrost tundra systems.

In conclusion, we find evidence that below-ground inputs of recently photosynthesized C result in RPEs that increase the age of mineralized SOC in permafrost soils in birch shrub and ericaceous heath tundra vegetation, but not in alder dominated vegetation. This implies that expansion of alder shrubs may lead to an increase in SOC accumulation rates in Arctic ecosystems, but expansion of birch shrubs may not. We argue that stimulation of SOC mineralization in soils in the presence of intact vegetation is the most likely explanation for the age shifts we observe, implying that below-ground allocation of recent photosynthate by birch and heath tundra vegetation accelerate the turnover of carbon that is >50 years old. Our results provide new evidence that plant allocation of recent photosynthate below-ground drives the turnover of SOC in permafrost systems.

#### ACKNOWLEDGEMENTS

We would like to thank the staff at the Aurora Research Institute in Inuvik, as well as Prof Philip Marsh and Prof Oliver Sonnentag, for providing logistical support and advice. We also thank Nancy Burns, Nicolas Pelletier, Ian Washbourne and Gwen Lancashire for their assistance with fieldwork.

#### CONFLICT OF INTEREST

The authors have no competing interests to declare.

#### AUTHOR CONTRIBUTION

L.E.S., P.A.W., J.-A.S. and M.H.G. conceived and designed the study. L.E.S., P.A.W., J.-A.S., J.F.D. and R.B. collected data in the field. L.E.S. analysed the data. All authors contributed to writing and editing the manuscript.

## DATA AVAILABILITY STATEMENT

All data are available as supplementary files.

## ORCID

Lorna E. Street  <https://orcid.org/0000-0001-9570-7479>  
 Mark H. Garnett  <https://orcid.org/0000-0001-6486-2126>  
 Jens-Arne Subke  <https://orcid.org/0000-0001-9244-639X>  
 Robert Baxter  <https://orcid.org/0000-0002-7504-6797>  
 Joshua F. Dean  <https://orcid.org/0000-0001-9058-7076>  
 Philip A. Wookey  <https://orcid.org/0000-0001-5957-6424>

## REFERENCES

- Berner, L. T., Jantz, P., Tape, K. D., & Goetz, S. J. (2018). Tundra plant above-ground biomass and shrub dominance mapped across the North Slope of Alaska. *Environmental Research Letters*, 13. <https://doi.org/10.1088/1748-9326/aaa9a>
- Bjorkman, A. D., Myers-Smith, I. H., Elmendorf, S. C., Normand, S., Rüger, N., Beck, P. S. A., ... Weiher, E. (2018). Plant functional trait change across a warming tundra biome. *Nature*, 562, 57–62. <https://doi.org/10.1038/s41586-018-0563-7>
- Blagodatskaya, E., & Kuzyakov, Y. (2008). Mechanisms of real and apparent priming effects and their dependence on soil microbial biomass and community structure: Critical review. *Biology and Fertility of Soils*, 45, 115–131. <https://doi.org/10.1007/s00374-008-0334-y>
- Blok, D., Heijmans, M. M. P. D., Schaepman-Strub, G., van Ruijven, J., Parmentier, F. J. W., Maximov, T. C., & Berendse, F. (2011). The cooling capacity of mosses: Controls on water and energy fluxes in a Siberian tundra site. *Ecosystems*, 14(7), 1055–1065. <https://doi.org/10.1007/s10021-011-9463-5>
- Burke, E. J., Chadburn, S. E., & Ekici, A. (2017). A vertical representation of soil carbon in the JULES land surface scheme (vn4.3-permafrost) with a focus on permafrost regions. *Geoscientific Model Development*, 10, 959–975.
- Burke, E. J., Ekici, A., Huang, Y. E., Chadburn, S. E., Huntingford, C., Ciais, P., ... Krinner, G. (2017). Quantifying uncertainties of permafrost carbon-climate feedbacks. *Biogeosciences*, 14, 3051–3066. <https://doi.org/10.5194/bg-14-3051-2017>
- Dean, J. F., Billett, M. F., Baxter, R., Dinsmore, K. J., Lessels, J. S., Street, L. E., ... Wookey, P. A. (2016). Biogeochemistry of “pristine” freshwater stream and lake systems in the western Canadian Arctic. *Biogeochemistry*, 130, 191–213. <https://doi.org/10.1007/s10533-016-0252-2>
- Dean, J. F., van der Velde, Y., Garnett, M. H., Dinsmore, K. J., Baxter, R., Lessels, J. S., ... Billett, M. F. (2018). Abundant pre-industrial carbon detected in Canadian Arctic headwaters: Implications for the permafrost carbon feedback. *Environmental Research Letters*, 13. <https://doi.org/10.1088/1748-9326/aaa1fe>
- Deslippe, J. R., & Simard, S. W. (2011). Below-ground carbon transfer among *Betula nana* may increase with warming in Arctic tundra. *New Phytologist*, 192, 689–698. <https://doi.org/10.1111/j.1469-8137.2011.03835.x>
- Dijkstra, F. A., Bader, N. E., Johnson, D. W., & Cheng, W. (2009). Does accelerated soil organic matter decomposition in the presence of plants increase plant N availability? *Soil Biology and Biochemistry*, 41(6), 1080–1087.
- Elmendorf, S. C., Henry, G. H. R., Hollister, R. D., Björk, R. G., Bjorkman, A. D., Callaghan, T. V., ... Wookey, P. A. (2012). Global assessment of experimental climate warming on tundra vegetation: Heterogeneity over space and time. *Ecology Letters*, 15, 164–175. <https://doi.org/10.1111/j.1461-0248.2011.01716.x>
- Garnett, M. H., & Hardie, S. M. L. (2009). Isotope ( $^{14}\text{C}$  and  $^{13}\text{C}$ ) analysis of deep peat  $\text{CO}_2$  using a passive sampling technique. *Soil Biology and Biochemistry*, 41, 2477–2483. <https://doi.org/10.1016/j.soilbio.2009.09.004>
- Garnett, M. H., & Murray, C. (2013). Processing of  $\text{CO}_2$  samples collected using zeolite molecular sieve for  $^{14}\text{C}$  analysis at the NERC radiocarbon facility (East Kilbride, UK). *Radiocarbon*, 55, 410–415.
- Gasser, T., Kechiar, M., Ciais, P., Burke, E. J., Kleinen, T., Zhu, D., ... Obersteiner, M. (2018). Path-dependent reductions in  $\text{CO}_2$  emission budgets caused by permafrost carbon release. *Nature Geoscience*, 11, 830–835. <https://doi.org/10.1038/s41561-018-0227-0>
- Gavazov, K., Albrecht, R., Buttler, A., Dorrepaal, E., Garnett, M. H., Gogo, S., ... Bragazza, L. (2018). Vascular plant-mediated controls on atmospheric carbon assimilation and peat carbon decomposition under climate change. *Global Change Biology*, 24, 3911–3921. <https://doi.org/10.1111/gcb.14140>
- Hardie, S. M. L., Garnett, M. H., Fallick, A. E., Rowland, A. P., & Ostle, N. J. (2005). Carbon dioxide capture using a zeolite molecular sieve sampling system for isotopic studies ( $^{13}\text{C}$  and  $^{14}\text{C}$ ) of respiration. *Radiocarbon*, 47, 441–451.
- Hartley, I. P., Garnett, M. H., Sommerkorn, M., Hopkins, D. W., Fletcher, B. J., Sloan, V. L., ... Wookey, P. A. (2012). A potential loss of carbon associated with greater plant growth in the European Arctic. *Nature Climate Change*, 2, 875–879. <https://doi.org/10.1038/nclimate1575>
- Hobbie, J. E., & Hobbie, E. A. (2006).  $^{15}\text{N}$  in symbiotic fungi and plants estimates nitrogen and carbon flux rates in arctic tundra. *Ecology*, 87, 816–822. [https://doi.org/10.1890/0012-9658\(2006\)87\[816:NISFAP\]2.0.CO;2](https://doi.org/10.1890/0012-9658(2006)87[816:NISFAP]2.0.CO;2)
- Högberg, P., Nordgren, A., Buchmann, N., Taylor, A. F. S., Ekblad, A., Högberg, M. N., ... Read, D. J. (2001). Large-scale forest girdling shows that current photosynthesis drives soil respiration. *Nature*, 411, 789–792. <https://doi.org/10.1038/35081058>
- Hugelius, G., Strauss, J., Zubrzycki, S., Harden, J. W., Schuur, E. A. G., Ping, C.-L., ... Kuhry, P. (2014). Estimated stocks of circumpolar permafrost carbon with quantified uncertainty ranges and identified data gaps. *Biogeosciences*, 11, 6573–6593. <https://doi.org/10.5194/bg-11-6573-2014>
- Huo, C., Luo, Y., & Cheng, W. (2017). Rhizosphere priming effect: A meta-analysis. *Soil Biology and Biochemistry*, 111, 78–84. <https://doi.org/10.1016/j.soilbio.2017.04.003>
- Koven, C. D., Schuur, E. A. G., Schädel, C., Bohn, T. J., Burke, E. J., Chen, G., ... Turetsky, M. (2015). A simplified, data-constrained approach to estimate the permafrost carbon-climate feedback. *Philosophical Transactions of the Royal Society A: Mathematical, Physical and Engineering Sciences*, 373(2054). <https://doi.org/10.1098/rsta.2014.0423>
- Kuzyakov, Y., Friedel, J. K., & Stahr, K. (2000). Review of mechanisms and quantification of priming effects. *Soil Biology and Biochemistry*, 32, 1485–1498. [https://doi.org/10.1016/S0038-0717\(00\)00084-5](https://doi.org/10.1016/S0038-0717(00)00084-5)
- Levin, I., & Heshaimer, V. (2016). Radiocarbon – A unique tracer of global carbon cycle dynamics. *Radiocarbon*, 42, 69–80. <https://doi.org/10.1017/S0033822200053066>
- Marsh, P., Onclin, C., & Neumann, N. (2002). Water and energy fluxes in the lower Mackenzie valley, 1994/95. *Atmosphere-Ocean*, 40(2), 245–256. <https://doi.org/10.3137/ao.400211>
- Mikan, C. J., Schimel, J. P., & Doyle, A. P. (2002). Temperature controls of microbial respiration in arctic tundra soils above and below freezing. *Soil Biology and Biochemistry*, 34, 1785–1795. [https://doi.org/10.1016/S0038-0717\(02\)00168-2](https://doi.org/10.1016/S0038-0717(02)00168-2)
- Mitchell, J. S., & Ruess, R. W. (2009).  $\text{N}_2$  fixing alder (*Alnus viridis* spp. *fruticosa*) effects on soil properties across a secondary successional chronosequence in interior Alaska. *Biogeochemistry*, 95, 215–229. <https://doi.org/10.1007/s10533-009-9332-x>
- Myers-Smith, I. H., Forbes, B. C., Wilkening, M., Hallinger, M., Lantz, T., Blok, D., ... Hik, D. S. (2011). Shrub expansion in tundra ecosystems: Dynamics, impacts and research priorities. *Environmental Research Letters*, 6(4). <https://doi.org/10.1088/1748-9326/6/4/045509>
- Natali, S. M., Watts, J. D., Rogers, B. M., Potter, S., Ludwig, S. M., Selbmann A-K., & Donatella, Z. (2019). Large loss of  $\text{CO}_2$  in winter observed across the northern permafrost region. *Nature Climate Change*, 9(11), 852–857.

- Parker, T. C., Subke, J.-A., & Wookey, P. A. (2015). Rapid carbon turnover beneath shrub and tree vegetation is associated with low soil carbon stocks at a subarctic treeline. *Global Change Biology*, 21, 2070–2081. <https://doi.org/10.1111/gcb.12793>
- Pinheiro, J. C., & Bates, D. M. (2009). *Mixed-effects models in S and S-PLUS*. New York: Springer-Verlag, 2000 edition.
- Rampton, V. N. (1988). Geological Survey of Canada. *Memoir*, 423, 98. <https://doi.org/10.4095/126937>
- Schädel, C., Schuur, E. A. G., Bracho, R., Elberling, B. O., Knoblauch, C., Lee, H., ... Turetsky, M. R. (2014). Circumpolar assessment of permafrost C quality and its vulnerability over time using long-term incubation data. *Global Change Biology*, 20, 641–652. <https://doi.org/10.1111/gcb.12417>
- Schuur, E. A. G., McGuire, A. D., Schädel, C., Grosse, G., Harden, J. W., Hayes, D. J., ... Vonk, J. E. (2015). Climate change and the permafrost carbon feedback. *Nature*, 520, 171–179. <https://doi.org/10.1038/nature14338>
- Shaver, G. R., Rastetter, E. B., Salmon, V., Street, L. E., van de Weg, M., Rocha, A. V., ... Williams, M. (2013). Pan-Arctic modelling of net ecosystem exchange of CO<sub>2</sub>. *Philosophical Transactions of the Royal Society B: Biological Sciences*, 368. <https://doi.org/10.1098/rstb.2012.0485>
- Sørensen, M. V., Strimbeck, R., Nystuen, K. O., Kapas, R. E., Enquist, B. J., & Graae, B. J. (2018). Draining the pool? Carbon storage and fluxes in three alpine plant communities. *Ecosystems*, 21, 316–330. <https://doi.org/10.1007/s10021-017-0158-4>
- Street, L. E., Dean, J. F., Billett, M. F., Baxter, R., Dinsmore, K. J., Lessels, J. S., ... Wookey, P. A. (2016). Redox dynamics in the active layer of an Arctic headwater catchment; examining the potential for transfer of dissolved methane from soils to stream water. *Journal of Geophysical Research: Biogeosciences*, 121, 2776–2792. <https://doi.org/10.1002/2016JG003387>
- Street, L. E., Subke, J. A., Baxter, R., Dinsmore, K. J., Knoblauch, C., & Wookey, P. A. (2018). Ecosystem carbon dynamics differ between tundra shrub types in the western Canadian Arctic. *Environmental Research Letters*, 13. <https://doi.org/10.1088/1748-9326/aad363>
- Stuiver, M., & Polach, H. A. (1977). Discussion reporting of <sup>14</sup>C data. *Radiocarbon*, 19, 355–363.
- Subke, J.-A., Ingle, I., & Francesca Cotrufo, M. (2006). Trends and methodological impacts in soil CO<sub>2</sub> efflux partitioning: A meta-analytical review. *Global Change Biology*, 12, 921–943. <https://doi.org/10.1111/j.1365-2486.2006.01117.x>
- Teare. (1998). *Spatial and temporal patterns of chemical solute signals in sixteen small tundra streams of the Trail Valley Creek watershed in the Western Canadian Arctic*. Vancouver: Simon Fraser University.
- Tokarska, K. B., & Gillett, N. P. (2018). Cumulative carbon emissions budgets consistent with 1.5 °C global warming. *Nature Climate Change*, 8, 296–299. <https://doi.org/10.1038/s41558-018-0118-9>
- Turetsky, M. R., Abbott, B. W., Jones, M. C., Walter Anthony, K., Olefeldt, D., Schuur, E. A. G., ... Sannel, A. B. K. (2019). Permafrost collapse is accelerating carbon release. *Nature*, 569, 32–34. <https://doi.org/10.1038/d41586-019-01313-4>
- Wild, B., Gentsch, N., Capek, P., Diáková, K., Alves, R. J. E., Bárta, J., ... Richter, A. (2016). Plant-derived compounds stimulate the decomposition of organic matter in arctic permafrost soils. *Scientific Reports*, 6(1). <https://doi.org/10.1038/srep25607>
- Wild, B., Schnecker, J., Alves, R. J. E., Barsukov, P., Bárta, J., Čapek, P., ... Richter, A. (2014). Input of easily available organic C and N stimulates microbial decomposition of soil organic matter in arctic permafrost soil. *Soil Biology and Biochemistry*, 75, 143–151. <https://doi.org/10.1016/j.soilbio.2014.04.014>
- Wilmking, M., Harden, J., & Tape, K. (2006). Effect of tree line advance on carbon storage in NW Alaska. *Journal of Geophysical Research, Biogeosciences*, 111. <https://doi.org/10.1029/2005JG000074>

#### SUPPORTING INFORMATION

Additional supporting information may be found online in the Supporting Information section.

**How to cite this article:** Street LE, Garnett MH, Subke J-A, Baxter R, Dean JF, Wookey PA. Plant carbon allocation drives turnover of old soil organic matter in permafrost tundra soils. *Glob Change Biol*. 2020;00:1–13. <https://doi.org/10.1111/gcb.15134>